Fabrication of silver nanocomposite films impregnated with curcumin for superior antibacterial applications

K. Varaprasad · K. Vimala · S. Ravindra ·
N. Narayana Reddy · G. Venkata Subba Reddy ·
K. Mohana Raju

Abstract Silver nanocomposite films are found to be very effective material for anti-bacterial application. In the present work, sodium carboxylmethyl cellulose silver nanocomposite films (SCMC SNCF) were tried for antibacterial applications. To enhance their applicability novel film-silver nanoparticle-curcumin composites have been developed. SCMC SNCF are developed from sodium carboxylmethyl cellulose (SCMC), N,N^I-methylenebisacrylamide (MBA) and silver nitrate solution. These films were characterized by FTIR, UV–visible, XRD, TGA, DSC and TEM techniques. The formed silver nanoparticles have an average particle size of ~ 15 nm as observed by transmission electron microscopy (TEM). Curcumin loading into SCMC SNCF is achieved by diffusion mechanism. The UV–Visible analysis indicated that higher encapsulation of curcumin in the films with higher SCMC content. Further, it was observed that the presence of silver nanoparticles in the films enhanced the encapsulation of curcumin indicating an interaction between them. Moreover, the antibacterial activity showed that the SCMC films generated with silver nanoparticles have a synergistic effect in the antimicrobial activity against *Escherichia coli* (*E. coli*). In order improve the healing efficacy as antibacterial agents, curcumin loaded with SCMC SNCFs were developed which showed significant inhibition of *E. coli*

K. Varaprasad (✉) · K. Vimala · S. Ravindra ·
N. Narayana Reddy · K. Mohana Raju
Synthetic Polymer Laboratory, Department of Polymer Science and Technology, Sri Krishnadevaraya University, Anantapur 515055, India
e-mail: varmaindian@gmail.com; prasadadc@gmail.com

G. Venkata Subba Reddy
Department of Microbiology, Sri Krishnadevaraya University, Anantapur, Andhra Pradesh 515055, India

growth than the silver nanoparticles and curcumin alone film. Therefore, the present study clearly provides novel antimicrobial films which are potentially useful in preventing/treating infections.

1 Introduction

Polysaccharides are the most popular polymeric materials to prepare nanoparticles for wound dressing [1, 2] and drug delivery applications [3–5] as they are highly stable, safe, nontoxic, hydrophilic and biodegradable materials which can be easily modified chemically. Therefore, in recent years, a large number of studies have been conducted on polysaccharides for their potential application as nanoparticle drug delivery systems as well as antibacterial applications [6–8].

Recently, silver-based nanostructure materials have gained much attention to control infections. The use of silver nanoparticles (AgNPs) has exhibited improved antibacterial properties than bulk silver due to high surface area and high fraction of surface atoms, leading to incorporating more NPs inside the bacteria and promoting its efficacy in a sustained manner. Water soluble polymer based biomaterials are capable of the combined antibacterial properties of AgNPs having no toxicity [9]. Basing on this, numerous polymers have been employed to prepare polymer-silver nanocomposites [10]. The combination of silver nanoparticles with water soluble biopolymers will produce new antimicrobials. Among the various biopolymers, Carboxymethyl cellulose is widely used in drug delivery and wound dressing applications. The reason is its biocompatibility, and biodegradable nature with enormous metal complexation capacity [11]. In particular, sodium carboxymethyl cellulose (SCMC) is currently used in oral, pharmaceutical formulations and as tablet binder as well as

metal stabilization properties which enhanced the biomedical applications [10, 12]. For these applications, it is important to have good stability of nanoparticles in films Vimala et al. [13] developed polysaccharide silver nanoparticle films for antibacterial applications. Cédric Chauvierre et al. [14] used the based on polysaccharide based poly(alkylcyanoacrylates) nanoparticle templates for drug delivery applications. We recently reported the studies on chitosen based silver nanoparticle films which possessed superior antibacterial activity [15].

The objective of this study was to improve the swelling and mechanical properties as well as improved wound dressing properties of film by generating of silver nanoparticles as shown in Scheme 1. The developed SCMC silver nanoparticles composite films were analyzed by of UV–Vis, fourier transform infrared (FTIR) spectrophotometric, thermogravimetric analysis (TGA), differential scanning calorimetry (DSC) and transmission electron microscopy (TEM) techniques. Curcumin (CM), a hydrophobic polyphenolic compound derived from the rhizome of the herb *curcuma longa*, possesses a wide range of biological activity including wound healing, anti-bacterial, anti-oxidant, anti-inflammatory and anti-cancer properties [16]. Hence, this compound was incorporated into SCMC SNCF to improve significantly the therapeutic antibacterial efficacy of the film. The effect of AgNPs and curcumin on the antibacterial activity of the films was studied.

2 Materials

Sodium carboxymethyl cellulose (SCMC), N,N^1-methylenebisacrylamide (MBA), ammonium persulfate (APS),

silver nitrate (AgNO₃) were obtained from Merck (Mumbai, India) and used as received.

2.1 Preparation of SCMC films

One gram of SCMC powder was dissolved in 100 ml of distilled water and stirred for 6 h. To this solution additionally 2.59 mM of 1% MBA and 21.91 mM of APS were added for strong network. The reactant solution was transferred immediately onto a Teflon sheet covered glass plate (dimensions: 100 mm length × 100 mm width × 3 mm height) and dried at 25°C for 12 h. Finally this film was cut into the required length and wreath for further studies. The film codes and the corresponding feed composition are listed in Table 1.

2.2 Preparation of SCMC nanocomposite films

The procedure of synthesis was described in Scheme 1. One gram of SCMC was dissolved in 100 ml distilled water and stirred for 6 h. To this, AgNO₃ solution (200 mg/10 ml distilled water), 2.59 mM of MBA solution and 21.91 mM of APS solution were added at 25°C. This solution was kept in the sunlight for 1 h. The colorless solution started turning to red, then brown and brownish indicating the formation of AgNPs. The solution was then poured onto Teflon covered glass plates and dried as explained earlier. Finally, the dried film was cut into the required size for further studies.

2.3 Swelling studies

Dried films were swollen in (100 ml) phosphate buffer (pH 7.4) solution at 25°C. The weight of swollen films was measured at equilibrium swelling after removing the

Scheme 1 Schematic diagram of formation of SCMC silver nanocomposite films and curcumin encapsulated SCMC silver nanocomposite films
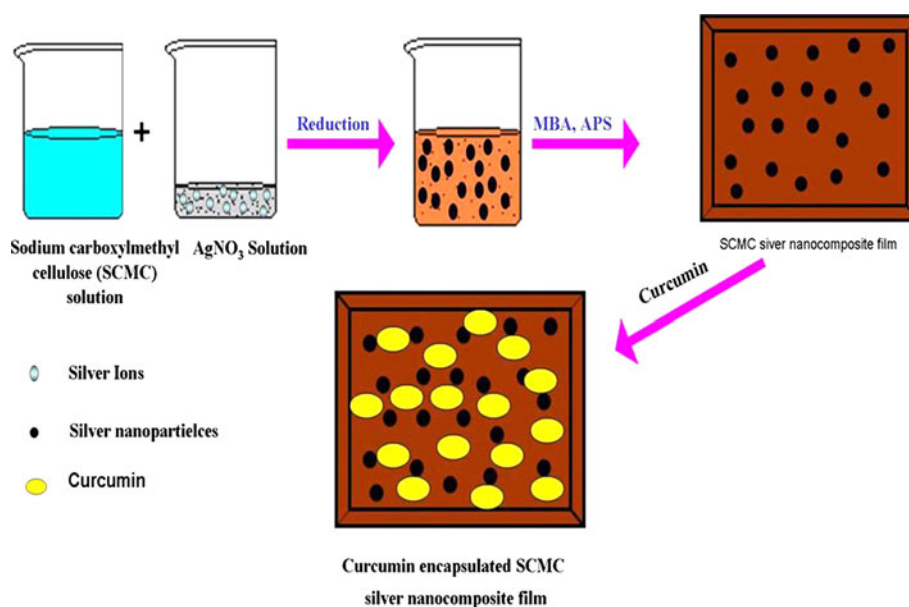
Table 1 Feed composition, mechanical properties and % of encapsulation efficiency and release kinetics parameters of hydrogels

Film code	Composition of components			Swelling data of films	
	SCMC (g)	MBA (mM)	APS (mM)	Swelling ratio (g/g)	SCMC-SNCF swelling ratio (g/g)
SCMC1	1	2.59	21.91	4.12	3.12
SCMC2	1.5	2.59	21.91	5.24	3.86
SCMC3	2	2.59	21.91	7.14	5.34
SCMC4	3	2.59	21.91	10.47	6.45

Mechanical properties of SCMC and SCMC SNCFs

Maximum stress (MPa)		Young's modulus (MPa)		Elongation at break (%)	
SCMC4	SCMC4 SNCF	SCMC4	SCCMC4 SNCF	SCMC4	SCMC4 SNCF
15.86	18.45	1496.00	1813.64	2.159	2.967

% of encapsulation efficiency and release kinetics parameters of different formulations at 25°C

Film code	% of encapsulation efficiency	n	k (10^2)	R^2	% of curcumin cumulative release at ambient temperatures at 30 min	% of curcumin cumulative releases at ambient temperatures at there end time
SCMC4-CM	46.25	0.86	0.4764	0.877	8.13	100
SCMC1-CM	31.53	0.98	0.5917	0.9712	4.13	100
SCMC4 SNCF-CM	71.25	1.38	1.70	0.99	1.97	90.73
SCMC1 SNCF-CM	43.98	1.62	2.37	0.98	1.08	74.74

surface solution with filter paper. Swelling ratio (Q) was calculated as follows: $Q = W_e/W_d$, where W_e is the weight of the swollen film at equilibrium and W_d is the dry weight of the film.

2.4 Characterization

2.4.1 FTIR spectroscopy

To record the FTIR spectra of films, the samples were completely dried in an oven at 40°C for 6 h. The spectra was recorded between 500 and 4000 cm^{-1} on a MB3000 Model, ABB company (Hoizon software) FTIR spectrometer (Quebec, Canada) using the KBr disk method.

2.5 Tensile test

The tensile parameters of the SCMC and SCMC SNCF samples were determined using the INSTRON 3369 Universal Testing Machine (Buckinghamshire, England). The specimens with dimensions of length 100 mm and width 10 mm were used. A gauge length of 50 mm was maintained for all the samples. The tensile parameters-maximum stress, modulus and % elongation at break were determined at a crosshead speed of 5 mm/min using a 10 kg load cell. In each case, three samples were used and the average value reported.

2.6 UV–Vis spectrophotometer

UV–Vis absorption spectra of the samples were recorded on a Shimadzu 160A model UV–Vis spectrophotometer in the range of 200–700 nm. For this study, 100 mg of silver nanocomposite film was dispersed in 10 ml of distilled water and allowed for 1 day to extract all silver nanoparticles into aqueous phase and these solutions were used for absorption spectra.

2.6.1 Transmission electron microscopy (TEM)

The size of the AgNPs in film network was determined using a Technai F12 TEM (Tokyo, Japan) microscope. For this study, the samples were prepared by placing a drop of aqueous solution of SCMC SNCF on carbon-coated copper grid and subsequently drying in air, before transferring them to the microscope operated at an accelerated voltage of 120 kV.

2.7 X-ray diffraction (XRD)

The X-ray diffraction method was used to identify the formation of nanoparticles in the films. These measurements were carriedout for dried and finely grounded samples on a Rikagu diffractometer (Cu radiation, $\lambda = 0.1546$ nm) running at 40 kV and 40 mA.

2.7.1 Thermogravimetric analysis (TGA)

The thermal analysis of pristine and AgNPs loaded films was carried on a SDT Q 600 TGA instrument (T.A. Instruments-water LLC, Newcastle, DE 19720, USA) at a heating rate of 10°C/min in 40–700°C range under a constant nitrogen flow (100 ml/min).

2.7.2 Differential scanning calorimetry (DSC)

Differential scanning calorimetry thermograms of pure curcumin(CM), AgNPs loaded film and curcumin loaded silver nanocomposite films were recorded using a SDT Q 600 DSC instrument (T.A. Instruments-water LLC, Newcastle, DE 19720, USA) at a heating rate of 10°C/min under a constant nitrogen flow (100 ml/min)in the temperature range of 40–450°C.

2.8 Curcumin loading and encapsulation efficiency

Curcumin (CM) is loaded into SCMC or SCMC SNCF films by swelling method. For loading curcumin, the films (50 mg) are allowed to swell in 20 ml of CM solution (5 mg of CM in 20 ml, acetone (8 ml)—distilled water (12 ml)) for 24 h at 25°C. The loading efficiency of curcumin in the films is determined spectrophotometrically [17]. The drug-loaded films are placed in 50 ml of buffer solution and stirred vigorously for 96 h to extract the drug from the films. The solution is filtered and assayed by UV spectrophotometer at fixed λ max value of 491.2 nm. The results of % drug loading and encapsulation efficiency are calculated using the following equations.

$$\% \text{ Drug loading} = (\text{Weight of drug in film}/ \text{Weight of film}) \times 100$$

$$\% \text{Encapsulation efficiency} = (\% \text{ actual loading }/ \% \text{ theoretical loading}) \times 100$$

2.9 In vitro drug release

The in vitro release studies of the CM drug were carried out by placing the dried and CM loaded film in definite volume (50 ml) of releasing medium (7.4 pH phosphate buffer) at 37°C. Drug release kinetics were analyzed by using the % of cumulative release data [18] (M_t/M_o) versus time (where M_t is the amount of drug released at time t and M_o is the initial loaded drug amount), the amount of CM released in pH 7.4 buffer was measured spectrophotometrically at λ_{max} 492.2 nm. Experimental results were fitted according to the following equation [19].

$$M_t/M_\infty = kt^n$$

where M_t/M_∞ is the faction released at time t and ∞ respectively, k is the apparent releases rate constant, and n is the diffusion exponent. The value of n determines the nature of the release mechanism, i.e. when $n = 0.5$ the release is Fickian diffusion mechanism and when n lies between 0.5 and 1, the release mechanism is anomalous in nature or Case II in nature. In addition if n being equal to 1, the mechanism is coined as Super Case II, the most desirable condition in controlled release technology [20–22].

2.10 Antibacterial activity

The antibacterial activity of the films prepared was investigated using two methods—disc method and count method.

2.10.1 Disc method

Nutrient agar medium was prepared by mixing peptone (5.0 g), beef extract (3.0 g), and sodium chloride (NaCl) (5.0 g) in 1000 ml distilled water and the pH was adjusted to 7.0. Finally, agar (15.0 g) was added to the solution. The agar medium was sterilized in a conical flask at a pressure of 15 lbs for 30 min. This medium was transferred into sterilized Petri dishes in a laminar air flow chamber (Microfilt Laminar Flow Ultra Clean Air Unit, India, Mumbai). After solidification of the media, E. coli and bacillus culture was spread on the solid surface of the media. To this inoculated Petri dish, one drop of gel solution (20 mg/10 ml distilled water) was added using 50-µl tip and incubated for 2 days at 37°C in the incubation chamber.

2.10.2 Count method

The effect of bacterial growth of E. coli in mineral salt medium (MSM) was studied in the presence of AgNPs or HSNCs. This medium was prepared by the following composition: NH_4NO_3 (1.5 g), KH_2PO_4 (2.5 g), K_2HPO_4 (0.5 g), NaCl (1.0 g), $MgSO_4$ (1.5 g), $MnSO_4$ (0.01 g), $FeSO_4$ (0.05 g), and $CaCl_2$ (0.05 g) and these were added to 1000 ml of distilled water and the pH was adjusted to 7.0. Then, yeast extract (0.01%) was added for bacterial growth. After that the MSM medium was sterilized, 50 ml of solution was transferred into a sterilized 250-ml conical flask. Afterward, 100 µl E. coli bacterium was added into the media. Finally, 100 µl of AgNP solution (20 mg/ 10 ml distilled water) or its equivalent AgNPs suspension was added, and the optical density of the bacterial medium was measured using a UV–vis spectrophotometer at 600 nm.

3 Results and discussions

The polymeric materials having silver nanoparticles have been a subject matter of numerous investigations because of their potential use in several applications, for instance, in wound/burn dressing [23]. For this reason, polymer films containing metal nanoparticles were directly employed in various biomedical fields. However, to improve further their applicability in wound/burn dressing, the present work was aimed in developing composite films containing silver nanoparticles (antimicrobial), and curcumin (wound healing). Here, we choose curcumin owing to its wound healing property, which is attributed to the presence of myofibroblast, and in enhancing fibronectin and collagen expression [23]. This combinational approach is expected to enhance their antibacterial efficacy. In the present study, natural polymeric films containing silver nanoparticles were developed by "green process". The advantages of this process are: (a) no need of extra reducing agent(s) and (b) process may be conducted at room temperature.

3.1 Swelling properties

The swelling capacity of the films is one of the important criteria for maintaining a moist environment over wound bed. Figure 1A illustrates the effect of SCMC content on the swelling property of the films. Figure 1Aa. indicates that the swelling capacity of the films was increased with increasing SCMC content in the films system. This behavior is attributed to the availability of more hydrophilic nature of SCMC (–OH) groups. This order is also same as in the case of SCMC films. The films (SCMC1-SCMC4) showed higher swelling capacity than silver nanocomposite films (SCMC SNCF) (Fig. 1Ab). The swelling ratio results (SCMC, SCMC SNCF) are parented in Table 1. This lowering in the swelling capacity can be attributed due to binding of AgNPs with electrons of 'O' and 'N' atoms of hydroxyl and amine groups present in SCMC/MBA chains thereby producing additional crosslink's within the chain networks [14].

3.2 UV–vis spectroscopy

In a series of SCMC SNCF, the AgNPs formation depends on the SCMC content. It is evident by UV–vis spectrophotometer that increase of SCMC content resulted increase in absorbance (0.75–2.79) of the characteristic band (451–462 nm) which arises from the surface plasmon absorbance of nanosized AgNPs. With the increase of SCMC content, the reduction capabilities as well as the stabilization of the formed nanoparticles increases due to presence of more number of hydrophilic (–OH) groups. The surface plasmon resonance absorption peak is observed (Fig. 1Bb) in between 451 and 462 nm indicating the formation of smaller AgNPs. The UV–vis spectrum of the SCMS films as well as AgNO$_3$ solution did not show any characteristic peak around 400–470 nm.

3.3 FTIR spectral analysis

FTIR spectroscopy is an important tool that indicates interaction between metal and polymer [24]. The spectra of SCMC and SCMC SNCF are shown in Fig. 2. The FTIR spectra of the SCMC film showed the typical absorption band at 1582.6 cm^{-1} corresponding to the stretching frequency of the COO$^-$ group. It is evident that the broad absorption band at 3338.3 cm^{-1} is due to the stretching frequency of the –OH group [25]. The band at 2918.7 cm^{-1} is due to C–H stretching vibration. The bands at around 1414.7 and 1320.85 cm^{-1} are assigned to –CH$_2$ scissoring and –OH bending vibration, respectively. The band at 1019.4 cm^{-1} is due to >CH–O–CH$_2$ stretching [9]. Whereas, Ag NPs loaded hydrogel film exhibited similar peak with slight change in their vibration frequencies [1591.6 (COO$^-$), 3254.7 (–OH), 2945.7 (–CH$_2$), and 1025.4 (–CH–O–CH$_2$)]. Therefore, all the above peaks found in the IR spectra of films confirm the presence of AgNPs in the SCMC SNCP film network.

3.4 TEM analysis

The transmission electron microscope (TEM) is a very versatile tool for probing the different aspects of nanostructure of metal nanoparticles (Gold, silver etc.). The TEM images have clearly revealed the formation of silver nanoparticles throughout the hydrogels network. The dark core should correspond to the metal silver. Electron diffraction pattern studies reveal a clear ring pattern for AgNPs (inset, Fig. 3A). From the TEM image, AgNPs have an average diameter of ∼15 nm. It can be concluded that these nanocomposites would release Ag NPs with time from SCMS film which can eventually prolong the antibacterial activity of Ag NPs.

3.5 XRD analysis

The X-ray diffraction (XRD) is used to evaluate the crystal structure of films that are widely used to confirm the formation of AgNPs (Fig. 3B). The plain film has not exhibited any sharp peaks in XRD pattern (Data not shown). In the case of silver nanocomposite film, sharp peaks are observed at 29.07, 31.89, 46.03, 56.10, and 76.63° Θ, which can be corroborated to (111), (200), (220), (222), and (311) reflections, due to the formation of metallic AgNPs in the film network.

Fig. 1 A Swelling behaviour of hydrogels (*a*) SCMC1-to-SCMC4, (*b*) SCMC1 to SCMC4 SNCF. **B** UV–Visible spectra (*a*) pure AgNO$_3$ solution and SCMC-plain film (*b*) silver nanocomposite films (SCMC1 SNCF-SCMC2 SNCF)
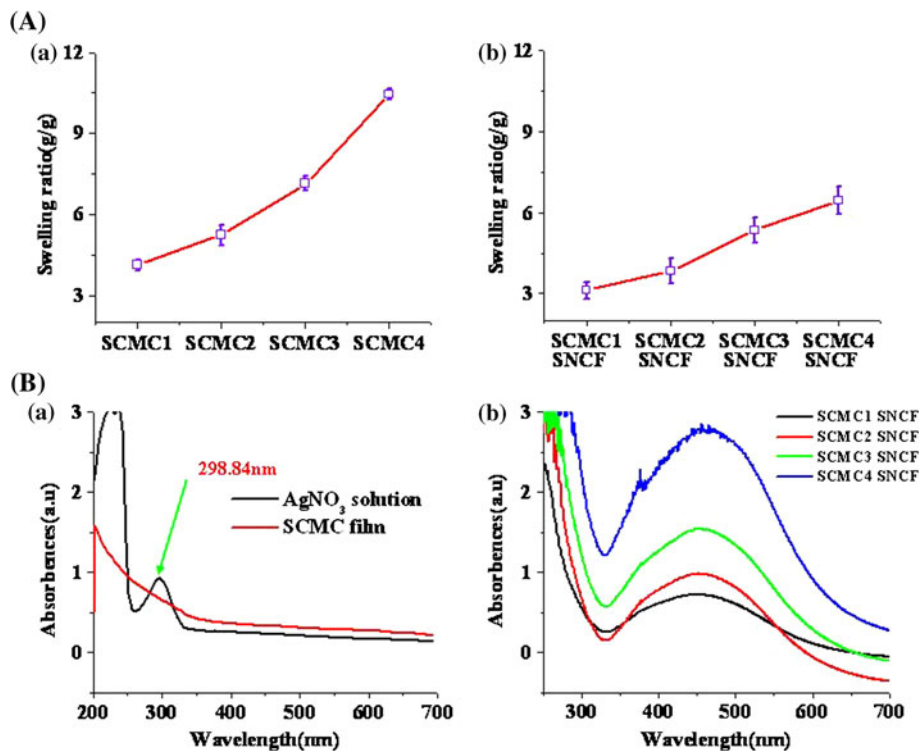

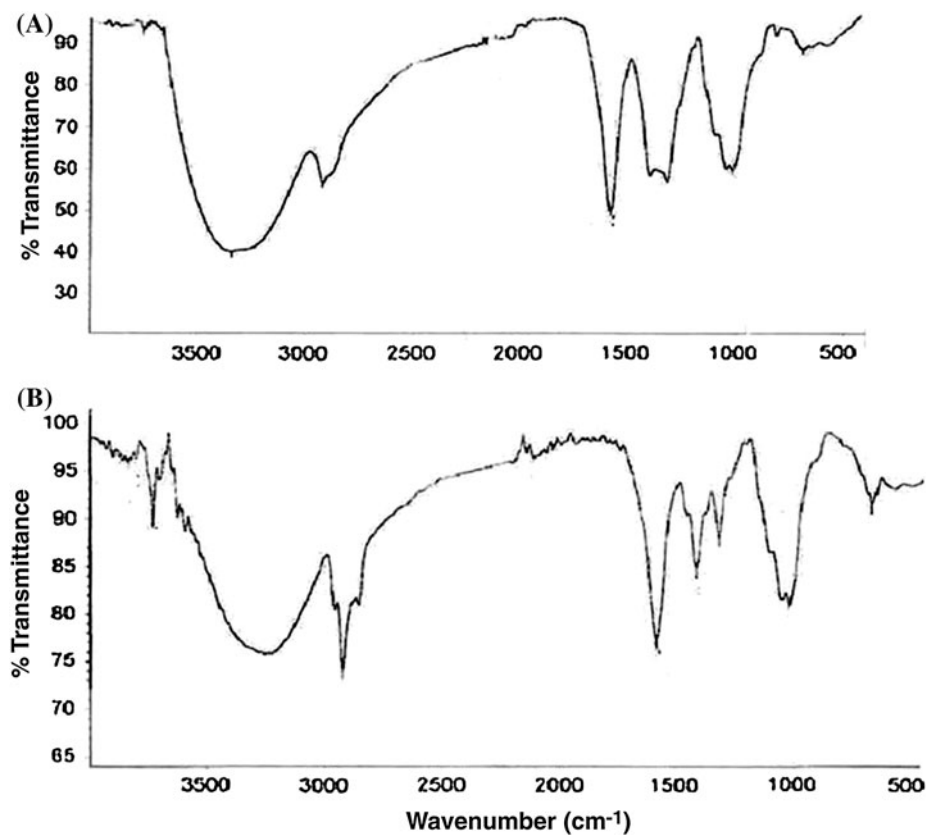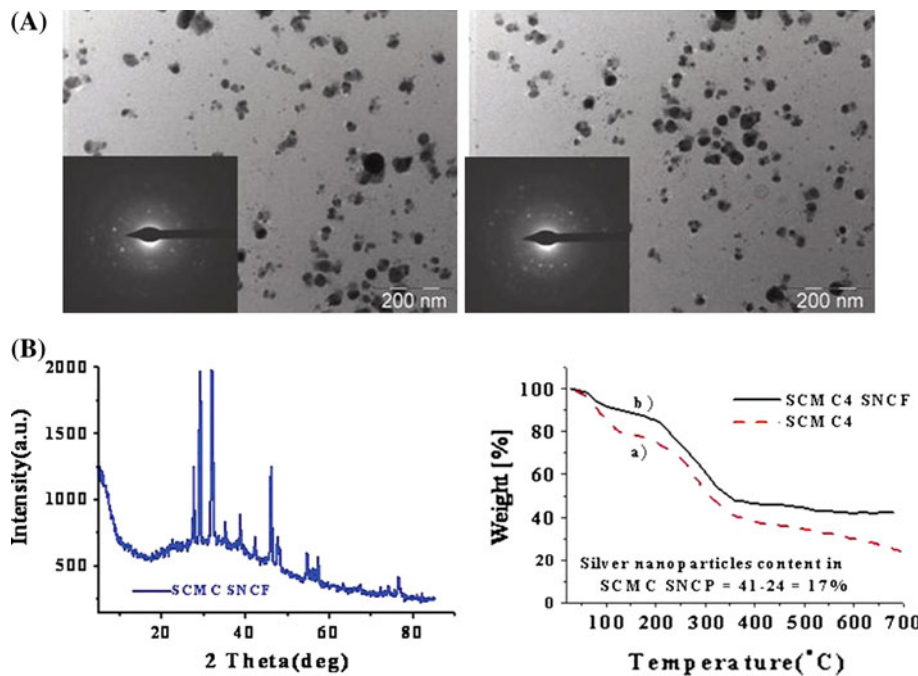**Fig. 2 a** FTIR spectra of SCMC2 film. **b** silver nanocomposite film (SCMC2 SNCF)

Fig. 3 **A** TEM images of silver nanoparticles film SCMC4 SNCF. **B** XRD patterns for SCMC4 SNCF. **C** Thermo gravimetric analysis of (*a*) plain (SCMC) and (*b*) silver nanoparticles loaded film

3.6 Thermo gravimetric analysis

The thermo-gravimetric analysis of the films (SCMC4 and SCMC4 SNCF) is presented in Fig. 3C. The initial weight loss observed at 80°C was attributed to the water molecules present. The weight loss observed in the case of SCMC4 film is 59.2% at 355°C whereas the weight loss observed for SCMC4 SNCP at this temperature is only 51.28%. From these studies, improved glass transition, melting temperatures and more residues at 700°C are obtained for AgNPs loaded films due to higher thermal stability of AgNPs. The % amount of AgNPs present in the SCMC4 SNCP film can be calculated from the difference in the weight loss between the SCMC4 and SCMC4 SNCP films at 700°C (which is 17.8%).

3.7 Mechanical properties

Figure 4 and Table 1 describe the mechanical analysis data for the pure sodium carboxyl methyl cellulose (SCMC4) and AgNPs loaded SCMC films (SCMC4 SNCF). The higher maximum stress, Young's modulus and elongation at break of the SCMC SNCF films were obtained than that of SCMC films. The main objective of this investigation is to produce higher strength SCMC SNCFs by impregnating AgNPs into film matrix.

3.8 Differential scanning calorimetry analysis

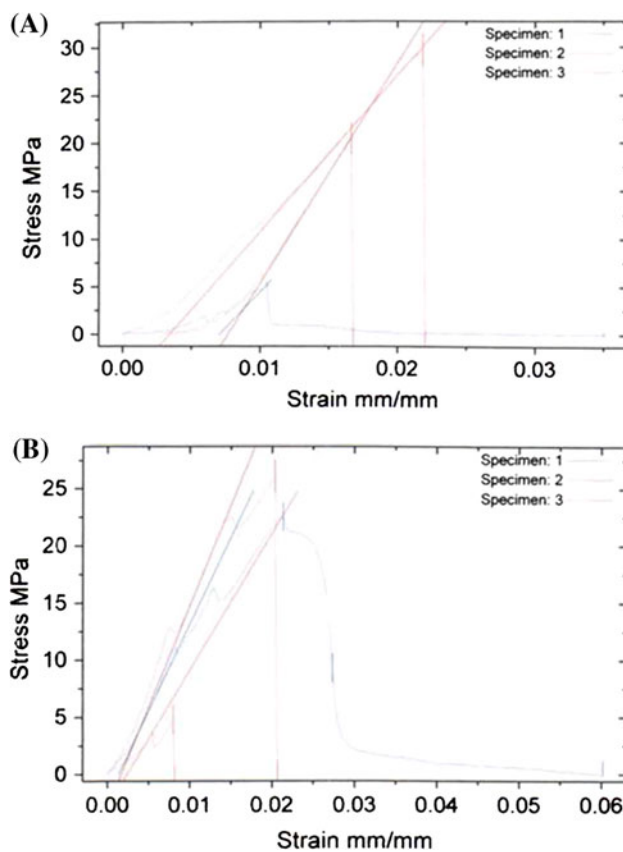DSC analysis of the pure CM, sliver loaded SCMC film and CM loaded SCMC SNCF are displayed in Fig. 6A.

Fig. 4 Uniaxial stress–strain curves of **a** SCMC2, and **b** SCMC2 SNCF films

However, because of the presence of curcumin, the curcumin loaded films have shown an additional peak between 175 and 182°C due to melting temperature of curcumin.

Therefore, DSC curve of the CM-loaded films suggest that CM is dispersed in the polymer matrix and also initial decomposition is higher in the case of SCMC SNCF compared to plain SCMC film.

3.9 Curcumin loading and release studies

The loading efficiency of curcumin into the hydrogels has been examined (Table 1). It is observed that the loading efficiency is higher in the case of SCMS SNCF film compared to SCMS films. This is due to absorption of more number of curcumin molecules on the silver nanoparticles in addition to entrapment in the films. Figure 5B and C gives the structure of curcumin and the drug delivery studies of SCMS and SCMS SNCF respectively.

In this study curcumin (CM) was selected as a model drug. CM is widely known for its anti-tumor, antioxidant, anti-inflammatory, anti-Alzheimer's, anti-cystic fibrosis, and wound-healing, properties [26–32]. Its chemical structure is shown in Fig. 6B. The percentage of cumulative release of CM from the films was calculated using the following equation.

The percentage of cumulative release
$$= M_t/M_o \times 100\%$$

where M_t is the amount of drug released at time t and M_o is the initial loaded drug amount. Figure 5C depicts the percentage of cumulative releases of CM from the films in 7.4 pH buffer solution at 37°C. The loading efficiency of CM into films is examined (Table 1). It can be understood that the loading efficiency is higher in the case of SCMC SNCP films compared to SCMC films. This is due to the presence of more number of CM molecules that are adsorbed on the AgNPs in addition to the entrapment in the films.

Kinetic data were processed (Experimental part) with an empirical relationship and the results are reported in Table 1. The values of n obtained from the kinetic analysis were in the range of 0.86–0.98 (plain SCMC films) and 1.38–1.62 (silver loaded SCMC films) which suggests anomalous nature and Super Case II release kinetic in pH media, respectively. The lower k values for all the systems indicate a lesser interaction between the film materials and the curcumin.

3.10 Antibacterial property test

The antibacterial activity is a demonstration of the release of silver nanoparticles from the polymer network such as hydrogels, films etc. Silver nanoparticles exhibit relatively large surface area, thus increasing their contact with bacteria. Silver nanoparticles show powerful bactericidal activity by binding with microbial DNA, thereby preventing
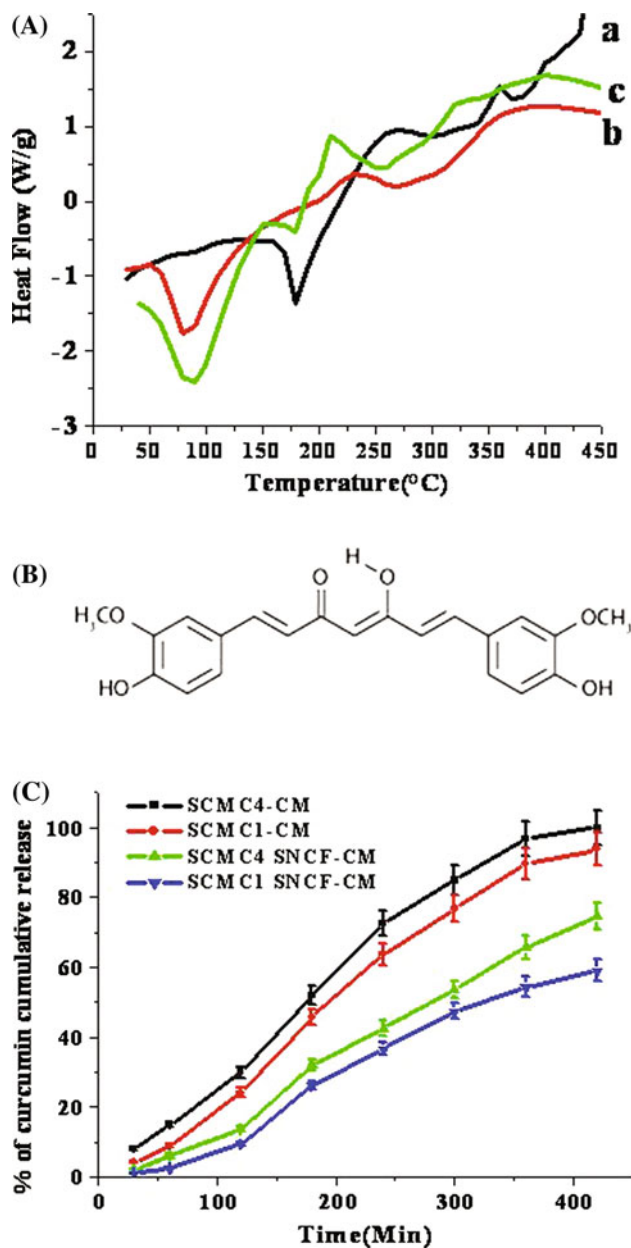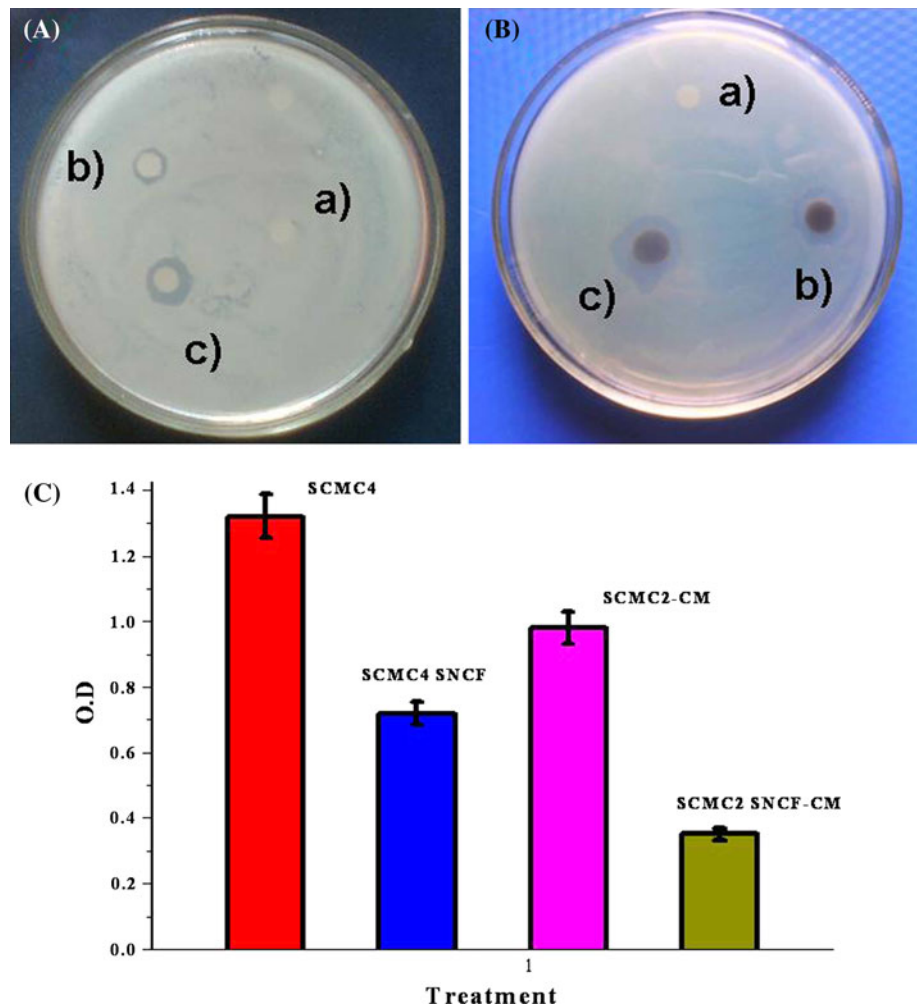

Fig. 5 **A** DSC termograms of (a) CM (b) silver nanocomposite film(SCMC2 SNCF) (c) CM loaded silver nanocomposite film(SCMC2 SNCF-CM). **B** Curcumin checimal stucture. **C** CM cumulative release profile of films

bacterial replication [33]. Similarly, Curcumin is a highly potent, nontoxic, bioactive agent found in turmeric and has been known for centuries as a household remedy to many ailments [16]. It has a number of pharmacological effects [34] especially in antibacterial [16].

Antimicrobial activity of pure, CM encapsulated film and CM encapsulated silver nanocomposite films, were evaluated from their capacity to inhibit bacterial cultures (Fig. 6). The inhibition zone (0.6 cm) is smaller for CM encapsulated pure (Fig. 6Ab) films and also AgNPs loaded film (0.9 cm)

Fig. 6 **A** Antibacterial activity of (*a*) Plain (SCMC3) film, (*b*) curcumin loaded (SCMC3) film and (*c*) curcumin loaded silver nanocomposite (SCMC3) film against *E. coli*. **B** Antibacterial activity of (*a*) plain (SCMC4) film, (*b*) silver nanocomposite (SCMC4 SNCF) film and (*c*) curcumin loaded silver nanocomposite (CM-SCMC4 SNCF) film against *E. coli*. **C** Semi-quantitative inhibition effects of SCMC based films against *E. coli*

system (Fig. 6Bb) compared with CM encapsulated silver nanocomposite (1.25 cm) film (Fig. 6Bc) due to the fact that the AgNPs as well as CM combination highly inhibited bacteria. The same phenomenon was observed in mineral salt medium (Fig. 6C). The growth rate or killing kinetics of the *E. coli* has been performed in mineral salt medium (MSM) and the results are determined by culture turbidity (OD) measurements. Because of the presence of more number of silver nanoparticles and curcumin, SCMC SNCF-CM composite showed 86% inhibition growth while other film composites showed only 25% inhibition growth of *E. coli* (Fig. 6C). The reason for this is two fold are the curcumin suppresses the growth of bacteria and second the release of silver nanoparticles from the films networks. Over all the addition of CM to AgNPs enhanced the antibacterial activity. The nanocomposites release Ag nanoparticles as well as curcumin with time which can eventually promote their antibacterial application. It can be inferred from the study of the curcumin loaded sodium carboxylmethyl cellulose–silver nanocomposite films could be used for antimicrobial and biomedical applications.

4 Conclusion

In this work we successfully obtained curcumin nanocomposite systems based on polysaccharides and silver nanoparticles. These composites were developed and characterized by spectral, thermal, X-ray diffraction, and electronic microscopic studies. The developed silver nanocomposite films exhibited fairly good mechanical strength and superior antimicrobial properties. Further, the current work demonstrates a promising method to combine silver nanocomposites with a natural compound (curcumin) in developing novel antimicrobial agents. These agents may find potential applications in antimicrobial packaging materials and wound/burns dressing.

References

1. Han Y-S, Lee S-H, Choi KH, Park I. Preparation and characterization of chitosan-clay nanocomposites with antimicrobial activity J Phys Chem Solids 2010;71:464–7.

2. Kiuchi H, Kai W, Inoue Y. Preparation and characterization of poly(ethylene glycol) crosslinked films. J Appl Polym Sci. 2008;107:3823–30.

3. Uhrich KE, Cannizzaro SM, Langer RS. Polymeric systems for controlled drug release. Chem Rev. 1999;99:3181.

4. Ranney DF. Biomimetic transport and rational drug delivery. Biochem Pharmacol. 2000;59:105–14.

5. Soppimath KS, Aminabhavi TM, Kulkarni AR. Biodegradable polymeric nanoparticles as drug delivery devices. J Control Release. 2001;70:1–20.

6. Lemarchand C, Gref R, Couvreur P. Polysacchride-decorated nanopartiecles. J Eur Pharm Biopharm. 2004;58:327–41.

7. Rubinstein A. Natural polysaccharides as targeting tools of drugs to the human colon. Drug Dev Res. 2000;50:435–9.

8. Sinha VR, Kumria R. Polysaccharides in colon-specific drug delivery. Int J Pharm. 2001;224:19–38.

9. Ma J, Xu Y, Fan B, Liang B. Preparation and characterization of sodium carboxymethylcellulose/poly(N-isopropylacrylamide)/clay semi-IPN nanocomposite hydrogels. J Eur Polym. 2007;43:2221.

10. Nadagouda MN, Varma RS. Systhesis of thermally stable carboxymethyl cellulose/metal biodegradable nanocomposites for potentia biological applications. Biomacromolecules. 2007;8:2762.

11. Choi Y, Simonsen J. Cellulose nanocrystal-filled carboxymethyl cellulose nanocomposites. J Nanosci Nanotech. 2006;6:633–9.

12. Ramirez Rigo MV, Allemandi DA, Manzo RH. Drug Deliv. 2009;16:108–15.

13. Chauvierre C, Manchanda R, Labarre D, Vauthier C, Marden MC, Leclerc L. Swellable drug—polyelectrolyte matrices of drug-carboxymethylcellulose complexes. Biomaterials 2010;31:6069–74.

14. Vimala K, Samba Sivudu K, Murali Mohan Y, Sreedhar B, Mohana Raju K. Controlled silver nanoparticles synthesis in semi-hydrogel networks of poly(acrylamide) and carbohydrates: a rational methodology for antibacterial application. Carbohyd Polym. 2009;75:47–463.

15. Vimala K, Murali Mohana Y, Samba Sivudua K, Varaprasada K, Ravindraa S, Narayana Reddya N, Padmab Y, Sreedharc B, Mohana Rajua K. Fabrication of porous chitosan films impregnated with silver nanoparticles: a facile approach for superior antibacterial application. Colloid Surf B: Biointerfaces. 2010;76:248–58.

16. Bhawana, Basniwal RK, Buttar HS, Jain VK, Jain N. Curcumin nanoparticles: preparation, characterization, and antimicrobial study. J Agric Food Chem. 2011;59:2056–61.

17. Suwantong O, Opanasopit P, Ruktanonchai U, Supaphol P. Electrospun cellulose acetate fiber mats containing curcumin and release characteristic of the herbal substance. Polymer. 2007;48:7546–57.

18. Ekici S, Saraydin D. Interpenetrating polymeric network hydrogels for potential gastrointestinal drug release. Polym Int. 2007;56:137.

19. Ritger PL, Peppas NA. A simple equation for description of solute release, II: Fickian and anomalous release from swellable devices. Control Release. 1987;5:37–42.

20. Lotfipour F, Nokhodchi A, Saeedi M, Norouzi-Sani S, Sharbafi J, Siahi-Shadbad MR. II Farmaco, The effect of hydrophilic and lipophilic polymers and fillers on the release rate of a tenolol from HPMC matrices. IL Farmaco. 2004;59:819–25.

21. Ranga Rao KV, Padmalatha Devi K, Buri P. Cellulose matrices for zero order release of soluble drugs. Drug Dev Ind Pharm. 1998;14:2299–320.

22. Talukdar MM, Kinget R. Swelling and drug release behaviour of xanthan gum matrix tablets. Int J Pharm. 1995;120:63–72.

23. Shahidi S, Rashidi A, Ghoranneviss M, Anvari A, Rahimi MK, Bameni Moghaddam M, Wiener J. Cellulose. 2010;17:627.

24. Varaprasad K, Murali Mohan Y, Ravindra S, Narayana Reddy N, Vimala K, Monika K, Sreedhar B, Mohana Raju K. Hydrogel–silver nanoparticle composites: a new generation of antimicrobials. J Appl Polym Sci. 2010;115:1199.

25. Biswal DR, Singh RP. Characterization of carboxymethyl cellulose and polyacrylamide graft copolymer. Carbohydr Polym. 2004;57:379–87.

26. Sharma RA, Gescher AJ, Steward WP. Curcumin: the story so far. J Eur Cancer. 2005;41:1955–68.

27. Jayaprakasha GK, Jagan L, Rao M, Sakariah KK. Trends Food Sci Tech. 2005;15:533.

28. Jayaprakasha GK, Rao LJ, Sakariah KK. Antioxidant activities of curcumin, demethoxycurcumin and bisdemethoxycurcumin. Food Chem. 2006;98:720.

29. Maheshwari RK, Singh AK, Gaddipati J, Srimal RC. Multiple biological activities of curcumin: a short review. Life Sci. 2006;78:2081.

30. Yang FS, Lim GP, Begum AN, Ubeda OJ, Simmons MR, Ambegaokar SS, Chen PP, Kayed R, Glabe CG, Frautschy SA, Cole GM. Curcumin inhibits formation of amyloid beta oligomers and fibrils, binds plaques, and reduces amyloid in vivo. J Biol Chem. 2005;280:5892.

31. Gopinath D, Ahmed MR, Gomathi K, Chitra K, Sehgal PK, Jayakumar R. Dermal wound healing processes with curcumin incorporated collagen films. Biomaterials. 2004;25:1911.

32. Jagetia GC, Rajanikant GK. Curcumin treatment enhances the repair and regeneration of wounds in mice exposed to hemibody gamma-irradiation. Plast Reconstr Surg. 2005;115:515.

33. Aggor FS, Ahmed EM, El-Aref AT, Asem MA. Synthesis and characterization of poly(Acrylamide-co-Acrylic acid) hydrogel containing silver nanoparticles for antimicrobial applications. J Am Sci. 2010;12:6.

34. Kaewnopparat N, Kaewnopparat S, Jangwang A, Maneenaun D, Chuchome T, Panichayupakaranant P. Increased solubility, dissolution and physicochemical studies of curcumin-polyvinylpyrrolidone K-30 solid dispersions. World Academy Sci, Eng Technol. 2009;55:229–34.